Behavior of Adhesive Anchors Reinforced with Postinstalled Steel Bars under Monotonic and Cyclic Loading*

Comportamiento de anclajes adhesivos reforzados con barras de acero posinstaladas ante cargas monotónicas y cíclicas

Diego Alberto Espitia Rojas
Pontificia Universidad Javeriana, Colombia
ORCID: https://orcid.org/0009-0009-0930-4346

Yezid Alexander Alvarado Vargas
Pontificia Universidad Javeriana, Colombia
ORCID: https://orcid.org/0000-0002-1260-8211

Daniel Mauricio Ruiz Valencia [a]
Pontificia Universidad Javeriana, Colombia
ORCID: https://orcid.org/0000-0003-4164-0357

DOI: https://doi.org/10.11144/Javeriana.iued28.baar

Received: 15 september 2024
Accepted: 27 november 2024
Published: 30 december 2024

Abstract:

This study analyzed the effectiveness of post-installed rebar with epoxy adhesive in increasing the load capacity of adhesive anchors under monotonic and cyclic tensile loading. The study analyzed anchor reinforcement alternatives for an installation case where the post-installed rebar had the same embedment depth as the original anchor. Monotonic tensile tests were performed to determine the percentage of load increase and to identify the best alternative through an efficiency analysis (additional load capacity/direct cost). In addition, cyclic tensile tests were performed to determine the load performance when the anchor was subjected to load and unload cycles. The optimal configuration, consisting of four #3 bars installed at a 55° angle, increased the monotonic load capacity by 25 % and the cyclic load capacity by 21 %. It was also shown that loading and unloading cycles affect the distribution of forces in the steel bars of the anchorage system. The results underscore the significant influence of bar diameter, number and angle on anchor performance and provide insight into cost-effective reinforcement strategies in adhesive anchorage systems.

Keywords: Adhesive Anchors, Anchor Reinforcement, Cyclic Loading, Monotonic Loading, Postinstalled Rebar.

Resumen:

Este estudio analizó la eficiencia de las barras de refuerzo posinstaladas con adhesivo epoxi para aumentar la capacidad de carga de los anclajes adhesivos bajo cargas de tracción monotónicas y cíclicas. El estudio analizó alternativas de refuerzo de anclajes para un caso de instalación en el que la barra de refuerzo posinstalada tenía la misma profundidad de empotramiento que el anclaje original. Se realizaron ensayos de tracción monotónica para determinar el porcentaje de incremento de carga e identificar la mejor alternativa mediante un análisis de eficiencia (capacidad de carga adicional / coste directo). Además, se realizaron ensayos de tracción cíclica para determinar el comportamiento de la carga cuando el anclaje se sometía a ciclos de carga y descarga. La configuración óptima, que consistió en cuatro barras #3 instaladas en un ángulo de 55°, aumentó la capacidad de carga monotónica en un 25 % y la capacidad de carga cíclica en un 21 %. También se demostró que los ciclos de carga y descarga afectan a la distribución de fuerzas en las barras de acero del sistema de anclaje. Los resultados subrayan la influencia significativa del diámetro, el número y el ángulo de las barras en el rendimiento de los anclajes y proporcionan información sobre estrategias de refuerzo rentables en los sistemas de anclaje adhesivo.

Palabras clave: anclajes adhesivos, reforzamiento de anclajes, cargas cíclicas, cargas monotónicas, barras de refuerzo posinstaladas.

Author notes

[a]Correspondence author. E-mail: daniel.ruiz@javeriana.edu.co

Introduction and Background

Adhesive anchors are important in the development of civil engineering projects. They allow flexibility in the planning, design, construction and strengthening of concrete structures [1][2]. Changes in use or codes require the design of postinstalled anchors that can withstand higher loads, but in many cases, they require effective embedment depths greater than the thickness of the concrete member in which they are to be installed. An alternative is to reinforce anchors by installing postinstalled reinforcing bars using epoxy adhesives that increase the tensile load capacity of the anchor [3][4]. This additional reinforcement may consist of stirrups, ties or fork heads placed at a distance less than or equal to $0.5h_{ef}$ (h_{ef} = effective embedment depth of the anchor) measured from the centerline of the anchor [5]. According to [6], when the anchor is subjected to tensile loading (Figure 1a), after cracking of the concrete, the stirrups are activated and resist the induced forces (Figure 1b). This behavior can be represented by the tensile strut model (Figure 1c), where the tensile load applied to the anchorage is transferred to a system of concrete struts that absorb the compressive forces (red color), whereas the stirrups and surface reinforcement resist the tensile forces (blue color) (Figure 1d) [6]. Vita et al. [3-6], Mousavi et al. [7-8] and Siamakani et al. [9] investigated the influence of varying the distance of the postinstalled bars (from the anchor centerline) between $0.35h_{ef}$ and $0.7h_{ef}$ the effective embedment depth of the reinforcing bars (between $1.5h_{ef}$ and $2.1h_{ef}$), the installation angle of the rebars, the number of rebars and their diameter for expansion and bonded anchors (Figure 2). Vita et al. [3] studied different configurations to understand the influence of postinstalled reinforcement (anchorage for M24 threaded bars). The results highlight that a relatively small number of postinstalled bars results in a significant increase in the anchorage capacity.

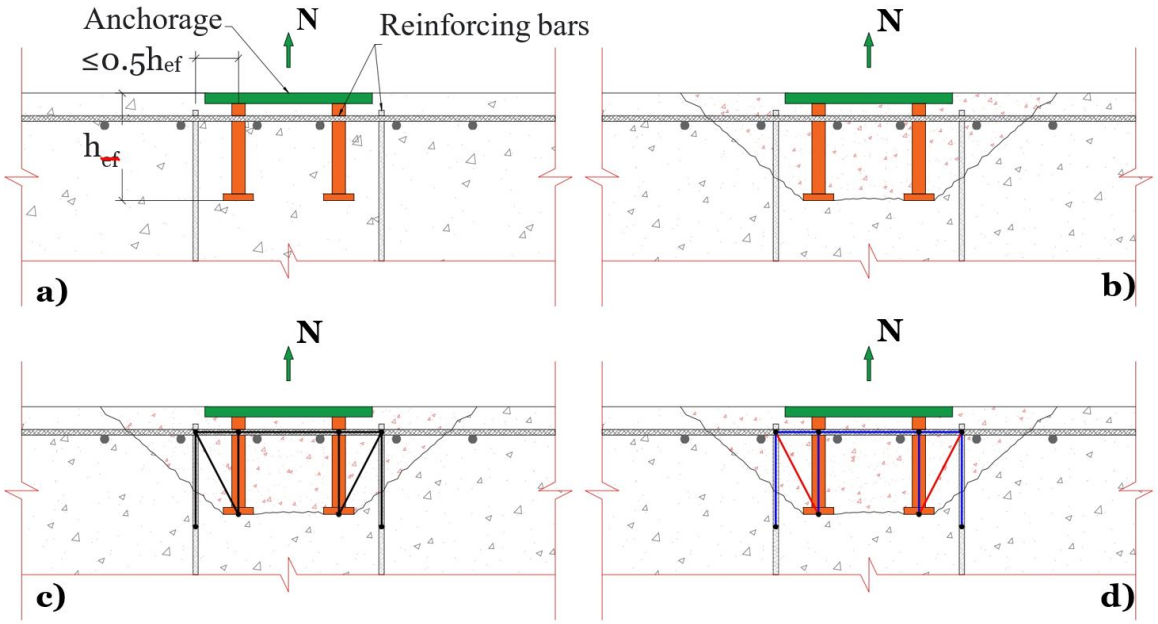

FIGURE 1
Tension strut model for anchors with preinstalled reinforcement (adapted from Vita et al. [6], American Concrete Institute [5]): a) system detail, b) system performance, c) tension strut model, and d) tension strut model analysis
Source: Own elaboration.

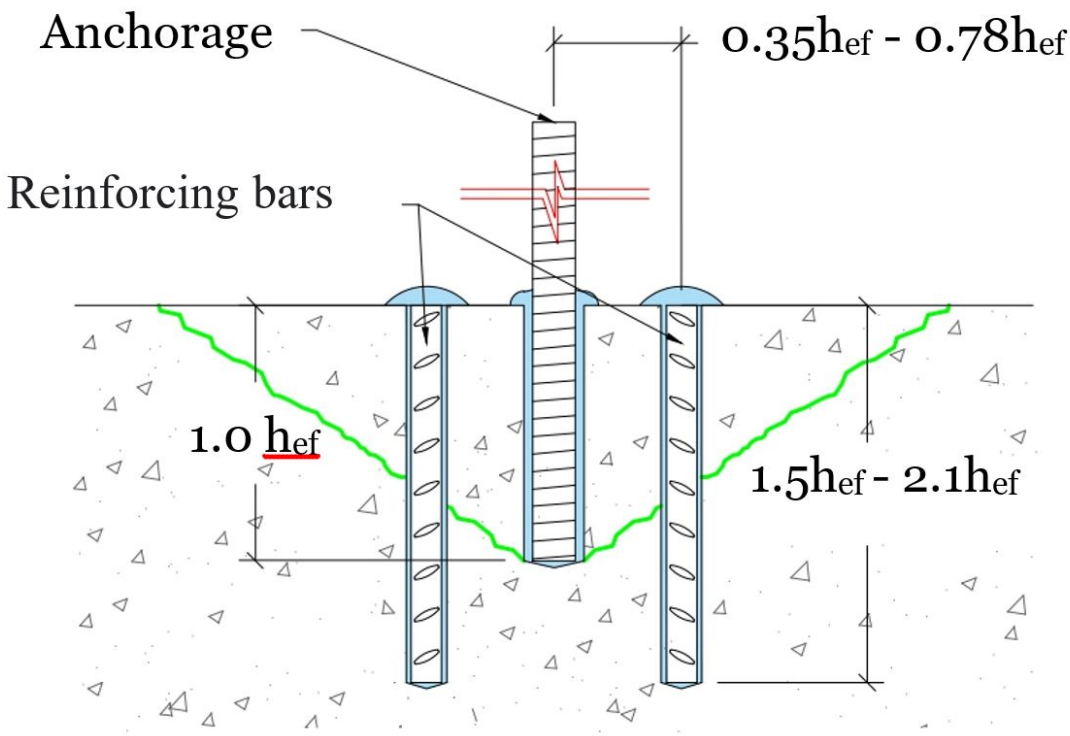

FIGURE 2
Bonded anchorage with postinstalled rebar
Source: Own elaboration.

Mousavi et al. [7] performed 18 monotonic unconfined tensile tests and concluded that anchors with postinstalled bars increased their load capacity by 144 % to 161 %. Mousavi et al. [8] performed 27 monotonic tensile tests for M12 and M20 threaded bar anchors with 12 mm diameter reinforcing bars. The authors concluded that the greater the number of reinforcing bars, the greater the increase in strength. Vita et al. [6] carried out tests on different variables that affect the behavior of a reinforced anchorage: the diameter of the postinstalled bars, the number of reinforcing bars, the installation angle, and the effective embedment depth, among others. Few studies have investigated the behavior of anchors reinforced with postinstalled reinforcing bars under cyclic tensile loading (Mahrenholtz et al. [10]). Considering the above background, the present research aimed to perform monotonic and cyclic unconfined tensile tests and to determine the influence of the number, diameter and installation angle of the postinstalled reinforcing bars for the case where the effective embedment depth of the postinstalled bars is equal to that of the main anchorage. In addition, the efficiency, measured as additional load capacity/cost, was determined.

Methodology

Experimental Program

In the first stage, unconfined (displacement-controlled) monotonic tensile tests were performed on eight postinstalled anchor reinforcement alternatives to determine the influence of the number, diameter and angle of installation of the reinforcement on the percentage change in load capacity ($N_{c\,\%\text{-}mo}$). Twenty-seven tests were performed, consisting of 3 tests on samples without postinstalled reinforcing bars (control samples, Figure 4a) and 24 samples for the reinforcement alternatives. These reinforcement alternatives were grouped

into 2 typologies such that the reinforcement was installed vertically (Figure 4b), with an effective depth of embedment of the reinforcing bars ($h_{ef\text{-}br}$) equal to the effective embedment depth for the threaded bar ($h_{ef\text{-}vr}$). For the remaining 4 alternatives, the reinforcement was installed at an angle of 55° with respect to the horizontal direction with a $h_{ef\text{-}br,}$ which does not exceed the $h_{ef\text{-}vr}$ measured vertically (Figure 4c). For these two groups, the number of reinforcing bars (2 or 4 bars) and their diameter were varied: No. 3 (i.e., 3/8 in=9.5 mm) or No. 4 (4/8 in = 13 mm). The distance of the bars measured from the main anchorage for the two groups was $0.5h_{ef\text{-}vr}$ (Figure 3).

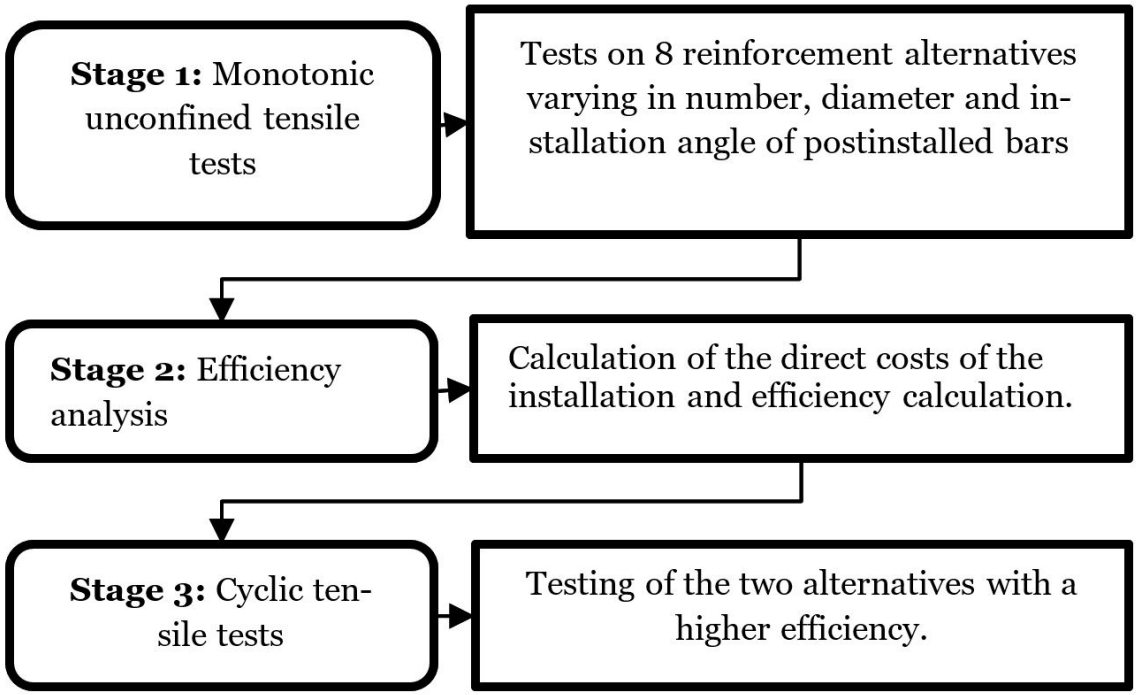

FIGURE 3
Flow chart of the methodology used
Source: Own elaboration.

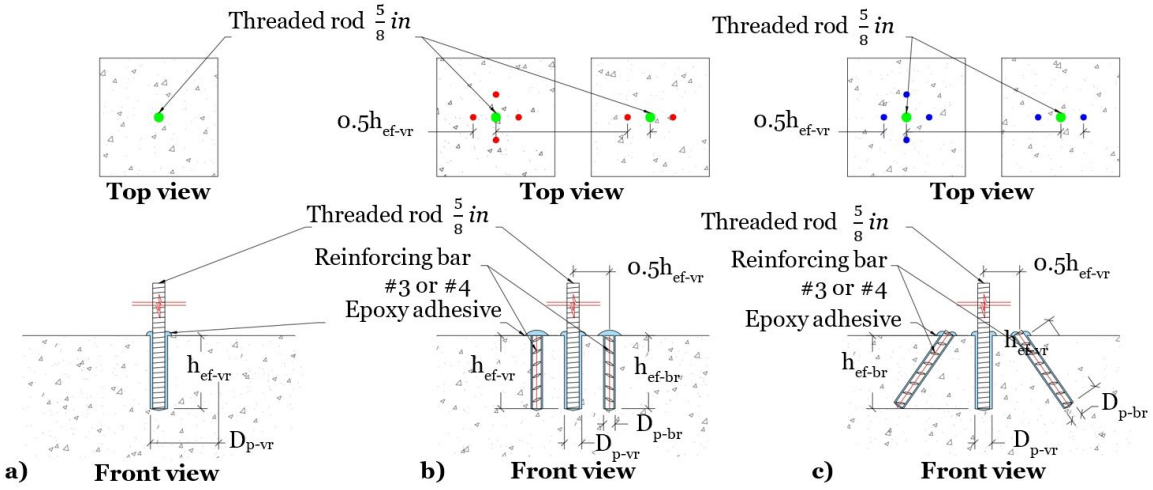

FIGURE 4
a) Case without reinforcement; b) case with reinforcement installed vertically; c) case with reinforcement installed at a 55° angle
Source: Own elaboration.

In the second step, the efficiency of each of the anchor reinforcement alternatives was evaluated in terms of additional load capacity per direct cost (e_{fic}). For each sample, the installation time for the reinforcement anchors was determined, and the direct cost of the reinforcement materials was calculated. The efficiency was subsequently calculated as the ratio between the additional load capacity and the direct cost. In the final stage, unconfined cyclic tensile tests were performed, and the test procedure consisted of two parts: first, force-controlled loading and unloading cycles were applied, and second, a monotonic load (displacement test) was applied until failure. This test was conducted for the two most efficient anchor reinforcement alternatives to determine the change in load capacity ($N_{c\,\%\text{-}cl}$) and its general behavior. Nine cyclic unconfined tensile tests were performed on the two most efficient reinforcement alternatives and the control sample.

Nomenclature of Test Samples

An alphanumeric nomenclature was assigned to each test case: M corresponds to the monotonic tension tests, CL corresponds to the cyclic tests, S corresponds to the control sample, A corresponds to the reinforcing bars installed at a drilling angle of 55° with respect to the surface, and V corresponds to the case where the reinforcing bars are installed vertically. The diameter of the No. 3 rebar was assigned #3, and the diameter of the No. 4 rebar was assigned #4. For the reinforcement case where there are two reinforcing bars, the nomenclature C2 was used, and for the case where there are four reinforcing bars, the nomenclature C4 was used. Finally, a consecutive number, starting from 1, was assigned to all the samples tested. For the installation of the anchors, concrete samples were prepared without reinforcing steel, with dimensions of 500 mm long to 500 mm wide and a thickness of 300 mm. These characteristics were in accordance with the guidelines proposed by ACI CODE-355.4 M-19(21) [11] and ASTM E488/E488M-22 [12], which ensured the free development of concrete cone failures (Figure 5).

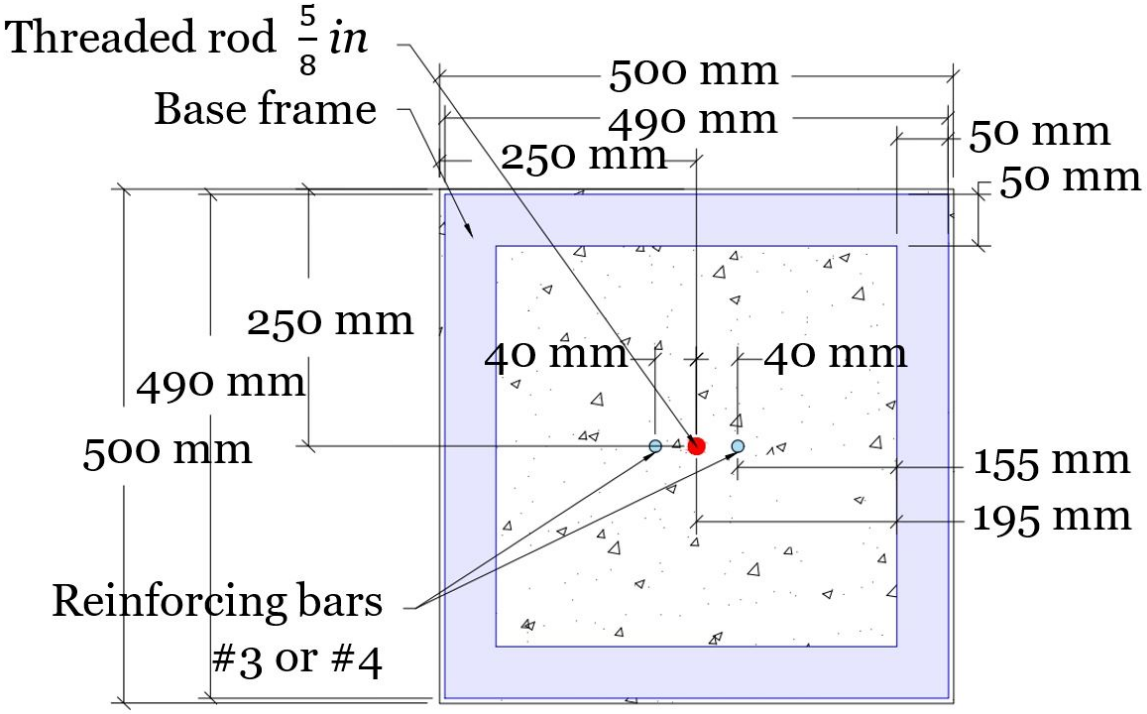

FIGURE 5
Sample dimensions in plain view
Source: Own elabotarion.

The main anchorage consisted of a 5/8 in (16 mm) diameter threaded rod with a $h_{ef\text{-}vr}$ embedded in 80 mm of concrete. For the installation of this element, a 19.1 mm diameter drill hole was made ($D_{p\text{-}vr}$ = diameter of the threaded rod). The anchor reinforcing bars were installed at $0.5h_{ef\text{-}vr}$, which is equivalent to 40 mm, and were measured from the center of the threaded bar. The $h_{ef\text{-}br}$ for the case of vertical installation was 80 mm, and for the case of installation at a 55° angle, it was 95 mm. A summary of the characteristics is provided in Table 1.

TABLE 1
General characteristics of the samples

Code	Number of tests	Effective embedment threaded rod $h_{ef\text{-}vr}$, mm	Drilling diameter for the threaded rod $D_{p\text{-}br}$, mm	Effective embedment depth Reinforcing bars $h_{ef\text{-}br}$, mm	Drilling diameter reinforcing bars $D_{p\text{-}br}$, mm (in)	Distance between threaded rod and reinforcing bars $0.5h_{ef\text{-}vr}$, mm
S	3	80	19.1 (3/4")	N/A	N/A	40
V-#3-C2	3			80	12.7 (1/2)	
V-#4-C2	3				15.9 (5/8)	
V-#3-C4	3				12.7 (1/2)	
V-#4-C4	3				15.9 (5/8)	
A-#3-C2	3			95	12.7 (1/2)	
A-#4-C2	3				15.9 (5/8)	
A-#3-C4	3				12.7 (1/2)	
A-#4-C4	3				15.9 (5/8)	

Source: Own elaboration.

Materials Characterization

The 5/8-inch (16 mm) diameter threaded bars were steel according to ASTM A193-06 B7 [13]. Reinforcing bars #3 (9.5 mm diameter) and #4 (12.7 mm diameter) were ASTM A706/A706M-22a [14]. The mechanical properties of the steel, such as yield stress (Fy), ultimate stress (Fu), and Young's modulus (E), were verified through tensile testing (ASTM E8/E8M-22 [15]) and are summarized in Table 2. A ready-mixed concrete with a maximum aggregate size of 19 mm and a design strength of 28 MPa at 28 days was used. The compressive strength of the concrete was determined according to ASTM C39/C39M:2021 [16], and the mechanical properties are summarized in Table 3 (15 tests). For the epoxy anchors, the mechanical properties of reference [17] were used.

TABLE 2
Mechanical properties of the steel bars

Type of bar	Number of samples	Fy [MPa]	Fu [MPa]	E [MPa]
Reinforcing bar No.3 (3/8 in)	3	453.2	645.1	213,958.6
Reinforcing bar No.4 (1/2 in)	3	458.1	620	214,544.9
Threaded rod 5/8 in	3	876.2	914.4	200,126.4

Source: Own elaboration.

TABLE 3
Mechanical properties of the concrete

Age of specimen [Days]	Compressive strength [MPa]	CoV [%]
28	31.5	1.8
48	31.1	6.6
56	29.6	3.2
140	29.4	7.7
142	29.8	3.7

Source: Own elaboration.

Installation Procedure

The threaded bar holes were drilled to a depth of 80 mm via a 2.9 J rotary hammer and a 19.1 mm diameter concrete drill. The #3 and #4 rebar holes were drilled with 12.7 mm and 16 mm diameter drills, respectively. A template was used to prevent movement during the installation process (Figure 6a). For the holes drilled at an angle of 55°, a guide was utilized and placed in the center of the sample (Figure 6b), and the hole was cleaned according to reference [18].

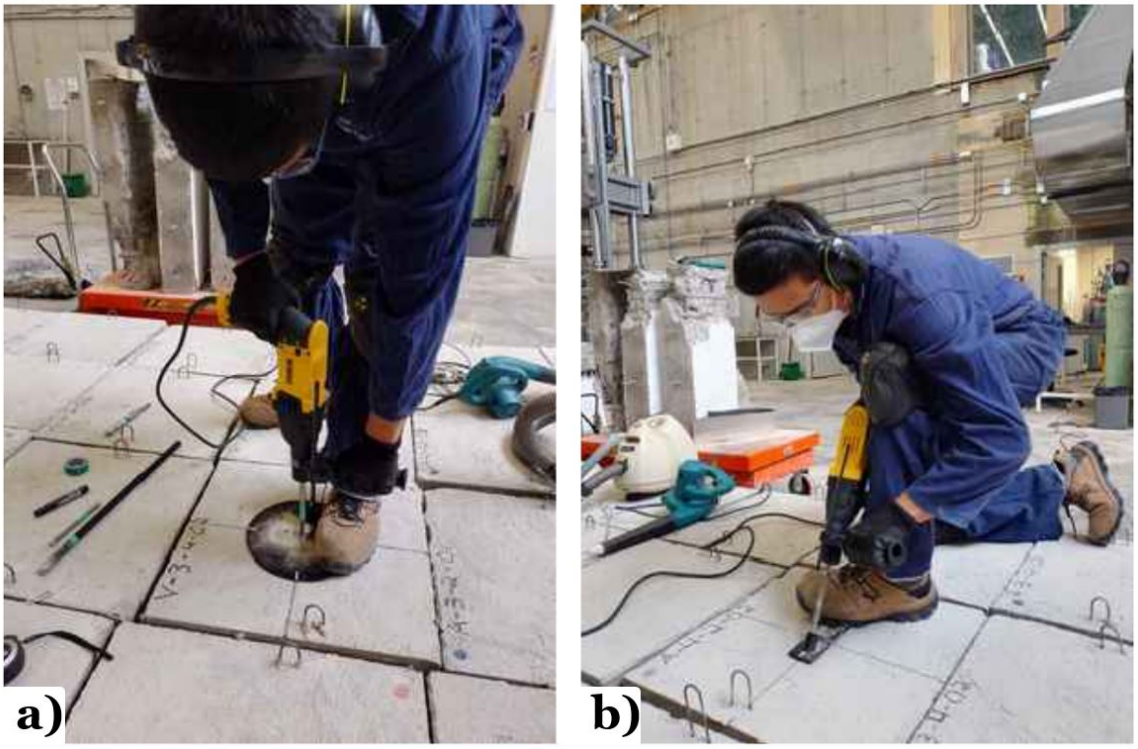

FIGURE 6
a) Vertical drilling process; b) Angled drilling process
Source: Own elaboration.

Similarly, strain gauges with a resistance of 120 Ω were installed at half the length of the effective embedment depth of the threaded rod and one of the rebars. Strain gauges were also installed on the control sample and two of the rebars.

Test Setup and Testing Method

The concrete sample was placed in the testing machine, and then, the sample was connected to the clamping frame (servo hydraulic testing MTS load frame 311.41). Next, two 50 mm stroke LVDTs (deformimeters) were installed, and the threaded rods were bolted to the base frame and machine base. A torque meter was employed to set the torque to 20 N-m for each threaded rod. The threaded rod was then clamped with the upper jaw of the machine, and a laser extensometer was installed to measure the deformation of the threaded rod. Finally, the gauges were connected (Figure 7). The test speed was 0.02 mm/s, which allows failure to occur between 1 and 3 minutes, according to ASTM E488/E488M-22 [12]. The data acquisition system was configured to record load damage, machine displacement, threaded bar deformation and anchor displacement simultaneously (at a sampling rate of 20 Hz). Unconfined cyclic tensile tests were also performed on the MTS load frame 311.41 frame. The ASTM E488/E488M-22 test procedure [12] consisted of subjecting the anchors to 150 cycles of sinusoidal loading and unloading tension at a frequency of 1 Hz with a minimum load magnitude of 5 kN and a maximum load magnitude of 57 kN. This maximum load was calculated as 90 % of the average maximum load ($N_{u\text{-}mo,m}$) for the sample without reinforcing bars (M-S) obtained from the monotonic tensile test. After the cyclic loading protocol was completed, a monotonic loading tensile test was performed. The cyclic test data acquisition system recorded the sensors at a rate of 100 Hz.

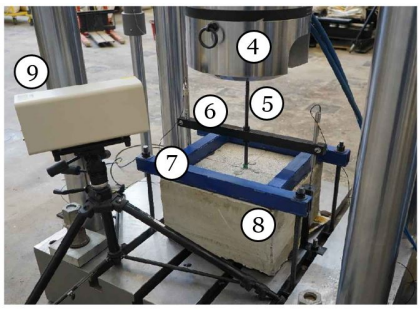

1) Servo-hydraulic testing MTS load frame 311.41
2) Data acquisition system
3) Load cell
4) Hydraulic jaw
5) Anchorage
6) Support for 2 LVDTs
7) Base frame
8) Concrete specimen
9) Laser extensometer

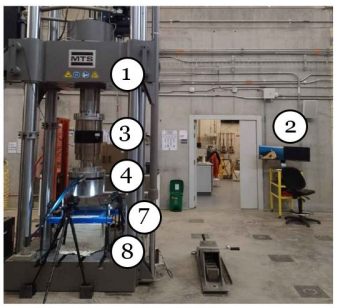

FIGURE 7
Test setup
Source: Own elaboration.

Results and Discussion

Monotonic Load Testing

Monotonic tensile tests were performed between Days 48 and 56. The results are presented in Table 4, which includes the following data: ultimate load ($N_{u\text{-}mo}$), the average maximum failure load per reinforcement alternative ($N_{u\text{-}mo,m}$), the coefficient of variation of the maximum failure load (CoV), displacement ($\delta_{a\text{-}mo}$), the average displacement for each reinforcement alternative ($\delta_{a\text{-}mo,m}$) and the type of failure observed. Table 5 summarizes the results obtained for the change in load carrying capacity ($N_{c\text{-}mo}$) and percentage change in carrying capacity ($N_{c\ \%\text{-}mo}$) for each reinforcement alternative. As shown in Table 6, the installation of reinforcing bars by any of the reinforcement alternatives increases the ultimate load capacity of the anchorage.

The greatest increase in the ultimate load capacity was obtained with the alternative (M-A-#3-C4), which demonstrated an increase of approximately 25 % in the load capacity.

TABLE 4
Results of monotonic tensile tests

Code	Maximum load, N_{u-mo} Test			Average $N_{u-mo,m}$ [kN]	COV [%]	Displacement, δ_{a-mo} Test			Average $\delta_{a-mo,m}$ [mm]	Type of failure Test		
	No.1 [kN]	No.2 [kN]	No.3 [kN]			No.1 [mm]	No.2 [mm]	No.3 [mm]		No.1	No.2	No.3
M-S	61.73	64.63	63.07	63.14	2.30	1.86	1.39	1.75	1.67	A	H+A	H+A
M-V-#3-C2	71.45	74.35	75.78	73.86	2.98	1.82	2.07	2.32	2.07	H+A	H+A	A
M-V-#4-C2	69.64	68.58	76.63	71.62	6.10	2.27	2.25	1.94	2.15	H+A	H	H
M-V-#3-C4	76.05	67.33	71.92	71.77	6.08	1.90	2.08	2.79	2.26	H+A	H+A	H+A
M-V-#4-C4	69.98	71.18	75.10	72.08	3.71	2.36	1.96	1.79	2.04	H	H	H
M-A-#3-C2	72.92	66.17	68.17	69.09	5.02	1.77	1.92	1.89	1.86	A	H	A
M-A-#4-C2	66.10	71.75	73.01	70.28	5.24	1.97	1.82	2.12	1.97	A	H	A
M-A-#3-C4	80.36	81.32	74.38	78.69	4.78	2.33	2.27	1.84	2.15	H+A	H+A	H+A
M-A-#4-C4	74.96	72.32	79.73	75.67	4.96	2.23	1.98	2.15	2.12	H	H+A	A

Note: A=Failure due to concrete pullout; H=Failure due to concrete spalling; H+A=Mixed failure.

Note. A = Failure due to concrete pullout; H = Failure due to concrete spalling; H+A = Mixed failure.
Source: Own elaboration.

TABLE 5
Change in the load capacity of the reinforced anchor

Code	Change in load capacity N_{c-mo} [kN]	Percentage change in load capacity $N_{c\ \%-mo}$ [%]
M-V-#3-C2	10.72	17.0%
M-V-#4-C2	8.48	13.4%
M-V-#3-C4	8.63	13.7%
M-V-#4-C4	8.94	14.2%
M-A-#3-C2	5.95	9.4%
M-A-#4-C2	7.14	11.3%
M-A-#3-C4	15.55	24.6%
M-A-#4-C4	12.53	19.8%

Source: Own elaboration.

Based on the studies reported in [19], the following three types of failure were identified in the tests: failure due to concrete pullout, failure due to concrete spalling, and a combination of the two types of failure mechanisms. As an example, Figure 8a shows the failure due to concrete pullout (framed in red) for the control sample.

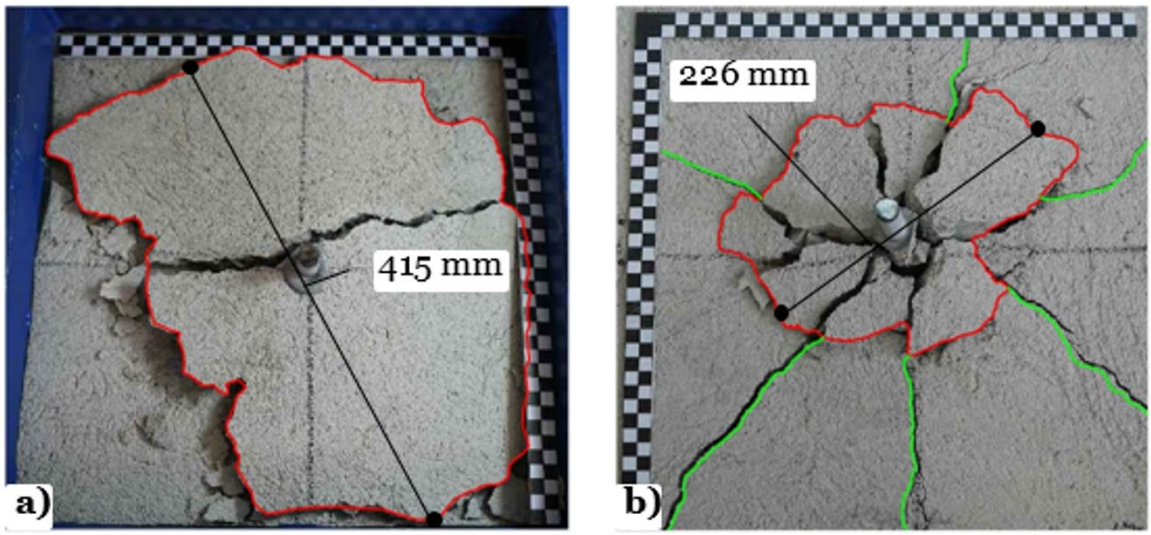

FIGURE 8
a) Concrete pull-out failure (M-S-01); b) mixed failure (M-S-02)
Source: Own elaboration.

Figure 9a illustrates the failure due to spalling for the alternative with two #4 reinforcing bars installed vertically, and Figure 9b shows the failure due to spalling for the alternatives with two #3 and #4 reinforcing bars installed at a 55° angle.

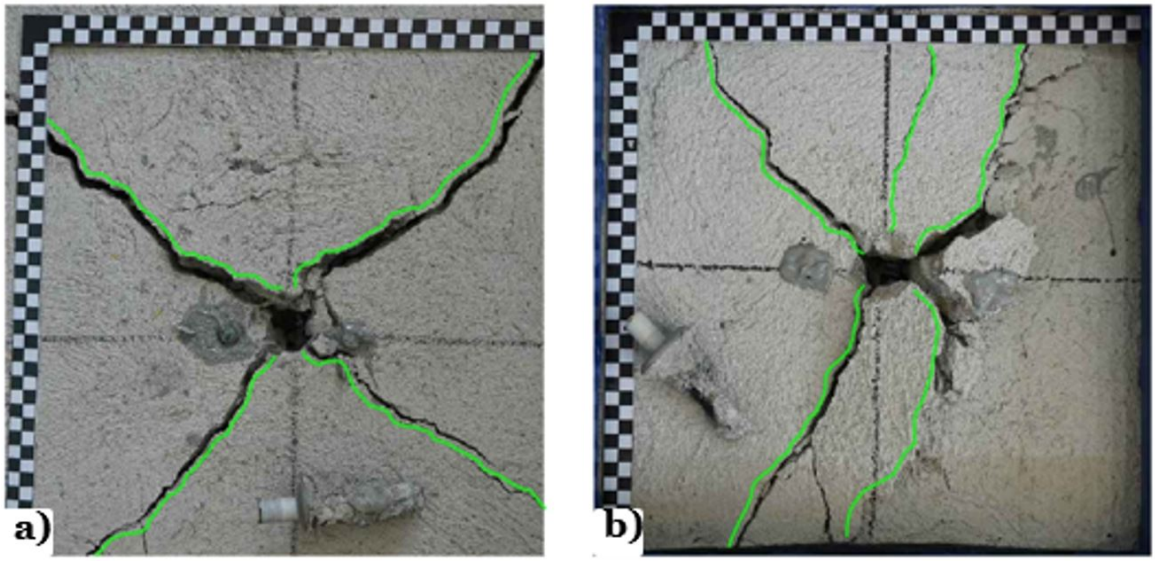

FIGURE 9
a) Failure due to concrete spalling (M-V-#4-C2-02); b) failure due to concrete spalling (M-A-#4-C2-02)
Source: Own elaboration.

Figure 10 shows the load-displacement curves for the M-V-#3-C2 and M-V-#3-C4 alternative tests compared with those of the M-S control sample tests. The percentage changes in the bearing capacity for alternatives M-V-#3-C2 and M-V-#3-C4 were 17 % and 13.7 %, respectively. The percentage changes in the bearing capacity for reinforcement alternatives M-V-#4-C2 and M-V-#4-C4 were 13.4 % and 14.2 %, respectively.

Regarding the influence of the diameter and number of postinstalled reinforcement bars with the inclination angle, Figure 11 shows a comparison of the load-displacement curves for the tests of control

specimen M-S and reinforcement alternatives M-A-#3-C2 and M-A-#3-C4. The percentage changes in the load capacity of alternatives M-A-#3-C2 and M-A-#3-C4 were 9.4 % and 24.6 %, respectively. Additionally, a comparison of the results between the tests of the control sample M-S and the reinforcement alternatives M-A-#4-C2 and M-A-#4-C4 revealed a percentage change in the load capacity of 11.3 % and 19.8 %, respectively.

Similarly, the influence of the installation angle of the postinstalled reinforcing bars was evaluated, and the maximum and minimum percentage changes in the anchorage load capacity of alternatives M-A-#3-C4 and M-A-#3-C2 were 24.6 % and 9.4 %, respectively. Likewise, when comparing the load-displacement results of the tests of the control specimen M-S and all the reinforcement alternatives, the curves of the alternatives in which the reinforcing bars were installed at an angle of 55° had an initial stiffness similar to that of the control sample; the opposite was the case for the curves of the alternatives in which the reinforcing bars were installed vertically.

An analysis of the secant stiffness of the samples was carried out considering the slope between the point of the maximum load and the initial point. The results are presented in Table 6. The data in this table show no significant differences between the configurations evaluated, with similar secant stiffness values ranging from 33 kN/mm to 38 kN/mm. In addition, the coefficients of variation (COVs) range from 5 % to 18 %, and it is statistically inconclusive whether one configuration has a higher stiffness than the average of the control samples.

TABLE 6
Stiffness of the samples tested

Code	Secant slope M_{-sec}			Average	COV
	Test			$M\text{-}sec_{,m}$	[%]
	No.1 [kN/mm]	No.2 [kN/mm]	No.3 [kN/mm]	[kN/mm]	
M-S	33.14	46.44	35.78	38.5	18%
M-V-#3-C2	39.36	35.98	32.71	36.0	9%
M-V-#4-C2	30.70	30.49	39.44	33.5	15%
M-V-#3-C4	40.37	32.47	25.75	32.9	22%
M-V-#4-C4	29.76	36.40	41.96	36.0	17%
M-A-#3-C2	41.10	34.70	35.84	37.2	9%
M-A-#4-C2	33.62	39.43	34.45	35.8	9%
M-A-#3-C4	34.63	35.85	40.55	37.0	8%
M-A-#4-C4	33.59	36.50	36.93	35.7	5%

Source: Own elaboration.

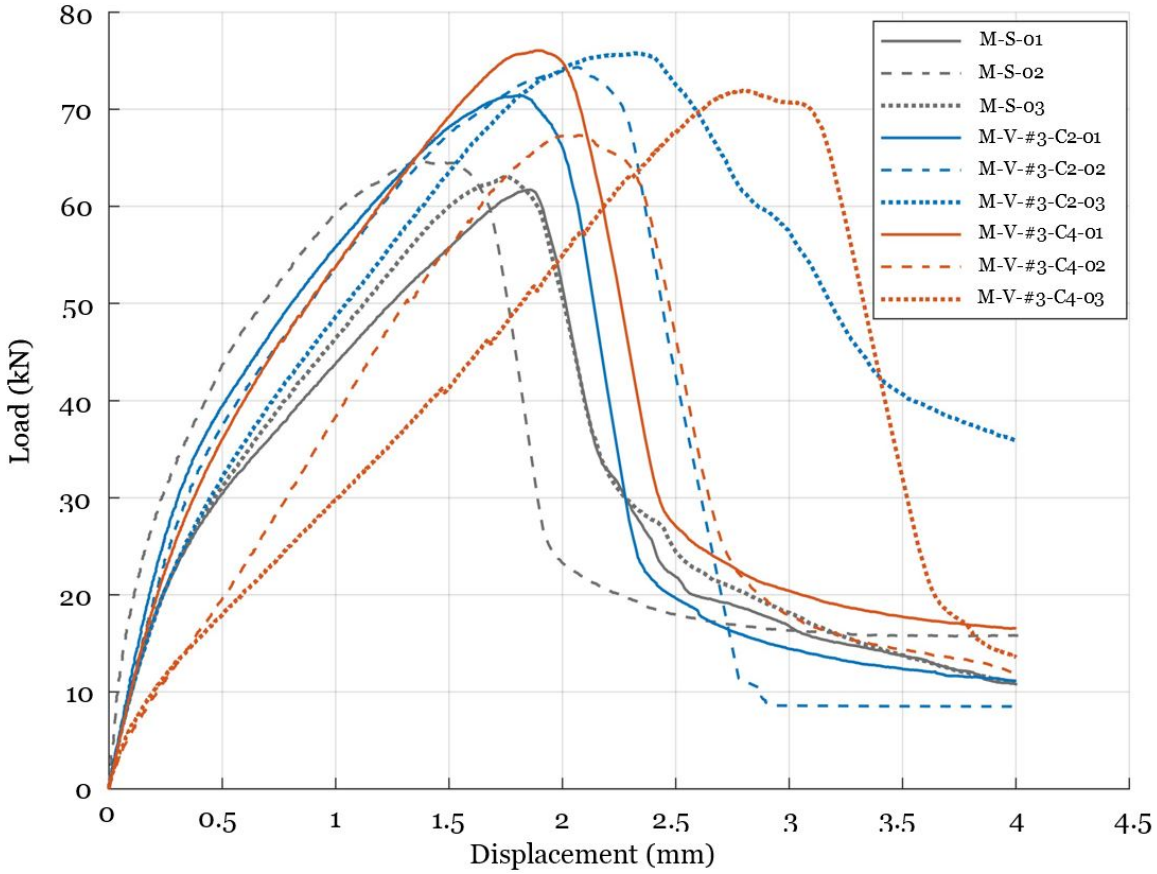

FIGURE 10
Load-displacement curves of anchors reinforced with two or four postinstalled vertical #3 reinforcing bars
Source: Own elaboration.

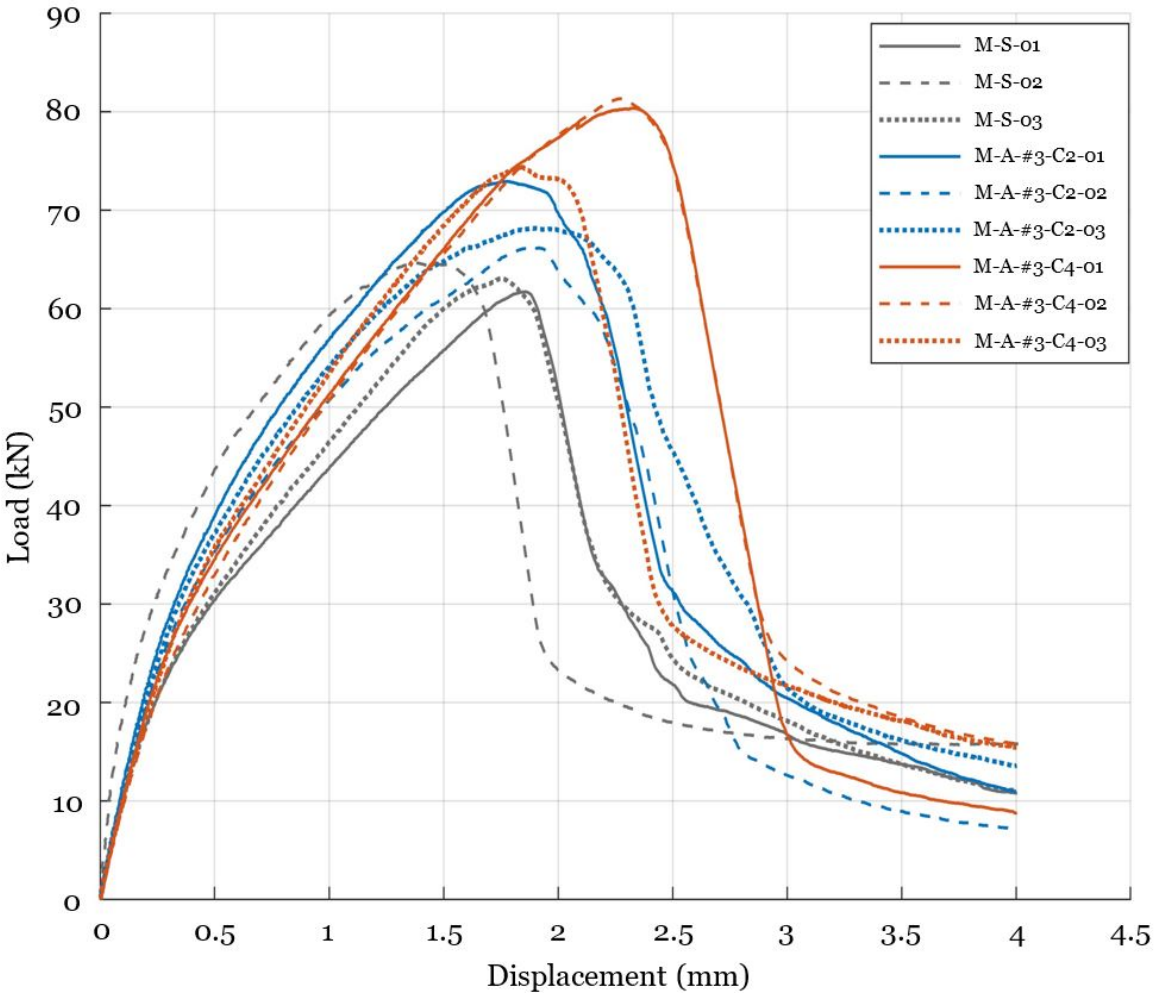

FIGURE 11
Load-displacement curves of an anchorage reinforced with two or four postinstalled #3 rebars at an angle of 55°
Source: Own elaboration.

Regarding the efficiency analysis, the results obtained by measuring the installation time for each reinforcement alternative ranged from 7 minutes (V-#3-C2) to 16 minutes (V-#4-C4). The cost of the installation time corresponds to the cost of one construction worker (2.52 USD per hour) [21]. Similarly, the cost of the reinforcing bars was determined from the price of a 6-meter-long rebar, which was 3.59 USD for bar #3 and 6.22 USD for bar #4. Similarly, the cost of the epoxy adhesive was determined using a price of $57.11 for an epoxy adhesive with a volume of 650 ml. A summary of the installation time cost, reinforcing bar cost, epoxy adhesive cost, and total direct cost for each reinforcement alternative is presented in Table 7.

TABLE 7
Direct cost of the installation

Code	Installation time (USD)	Reinforcing bar (USD)	Epoxy adhesive (USD)	Total direct cost (USD)
V-#3-C2	0.32	0.1	1.08	1.50
V-#4-C2	0.39	0.17	1.4	1.96
V-#3-C4	0.62	0.19	2.16	2.97
V-#4-C4	0.68	0.33	2.79	3.80
A-#3-C2	0.37	0.11	1.33	1.81
A-#4-C2	0.32	0.2	1.65	2.17
A-#3-C4	0.68	0.23	2.67	3.58
A-#4-C4	0.66	0.39	3.3	4.35

Source: Own elaboration.

Table 8 shows the efficiency calculation, which is defined as the ratio between the change in load capacity and the total direct installation cost. The highest numerical value represents the most efficient alternative. The two alternatives with the highest efficiency were V-#3-C2 and A-#3-C4, for which indicators of increase in resistance per unit cost were calculated to be 7.15 kN/USD and 4.34 kN/USD, respectively.

TABLE 8
Efficiency analysis

Code	Change in load capacity/cost e_{fic} kN/USD
V-#3-C2	7.147
V-#4-C2	4.321
V-#3-C4	2.906
V-#4-C4	2.353
A-#3-C2	3.282
A-#4-C2	3.29
A-#3-C4	4.344
A-#4-C4	2.88

Source: Own elaboration.

Cyclic Loading Tests

Cyclic tensile tests were performed between Days 140 and 142 from the date on which the concrete was cast. A total of nine tests were conducted, and the resulting data are summarized in Tables 9 and 10: the maximum failure load ($N_{u\text{-}cl}$) for each sample, the average maximum failure load per reinforcement alternative ($N_{u\text{-}cl,m}$), the coefficient of variation of the maximum failure load (CoV), the average displacement for each reinforcement alternative ($\delta_{a\text{-}cl,m}$), and the type of failure observed and the percentage change in the load carrying capacity ($N_{c\ \%\text{-}cl}$) for each reinforcement alternative. Notably, the samples with strain gages are also indicated with the symbol "*". When comparing the load-displacement results for the tests of alternatives CL-V-#3-C2 and CL-A-#3-C4 with the tests of the sample without reinforcing bars CL-S, a percentage change in the load capacity of alternatives CL-V-#3-C2 and CL-A-#3-C4 of 12.9 % and 21 %, respectively, was observed.

TABLE 9
Results of the cyclic tensile tests

Code	Maximum load $N_{u\text{-}cl}$ Test No.1 [kN]	Test No.2 [kN]	Test No.3 [kN]	Average $N_{u\text{-}cl,m}$ [kN]	COV [%]	Average displacement δa-cl,m [mm]
CL-S	73.23	69.09	72.33*	71.55	3.04	1.78
CL-V-#3-C2	80.22*	81.64	80.37	80.75	0.97	2.06
CL-A-#3-C4	86.15	84.69	88.91*	86.58	2.47	2.46

Source: Own elaboration.

Figure 12 shows the load-displacement graphs of the first part of the cyclic test in terms of the force applied by the MTS-load frame and the force supported by the threaded rod (CL-S-03). As shown in these two graphs, the force curve of the threaded rod is in the elastic region. Moreover, the curve of the force applied by the machine shows a displacement that increases as the test progresses, which is probably due to the damage that begins to accumulate in the concrete (Figure 13) and in the epoxy adhesive (Figure 14) due to cracking.

TABLE 10
Results of the cyclic tensile tests

Code	Type of failure Test No.1	Test No.2	Test No.3	Change in load capacity $N_{c\text{-}mo}$ [kN]	Percentage change in load capacity $N_{c\ \%\text{-}mo}$ [%]
CL-S	H+A	A	A	-	-
CL-V-#3-C2	H	H	H+A	9.2	12.9
CL-A-#3-C4	A	A	H+A	15.03	21

Note. A = concrete pull-out failure; H = concrete spalling failure; H+A = mixed failure. * = Strain gage instrumented samples on a threaded rod and one reinforcing bar.
Source: Own elaboration.

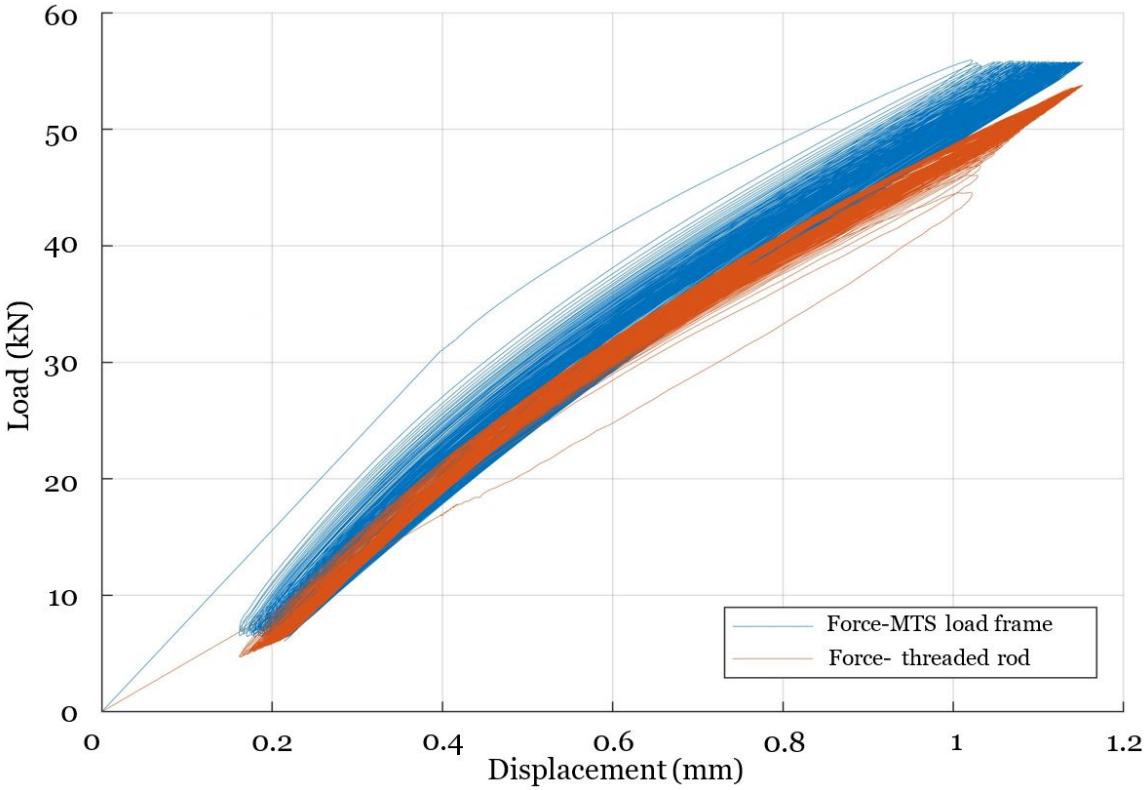

FIGURE 12
Load-time curves of anchorages without postinstalled reinforcing bars CL-S-03
Source: Own elaboration.

FIGURE 13
Concrete cracking during the application of load/unload cycles
Source: Own elaboration.

Figure 15 shows the load vs. time curve for the test of control specimen CL-S-03, where the force of the threaded rod is not equal to the force applied by the MTS load frame throughout the test. This difference is estimated to start at 8 kN and decreases until it reaches 2 kN. Moreover, it is observed that the force curve of the rod is disrupted, which is due to possible damage to the strain gage in the last part of the experimental test.

FIGURE 14
Epoxy adhesive cracks during loading and unloading cycles
Source: Own elaboration.

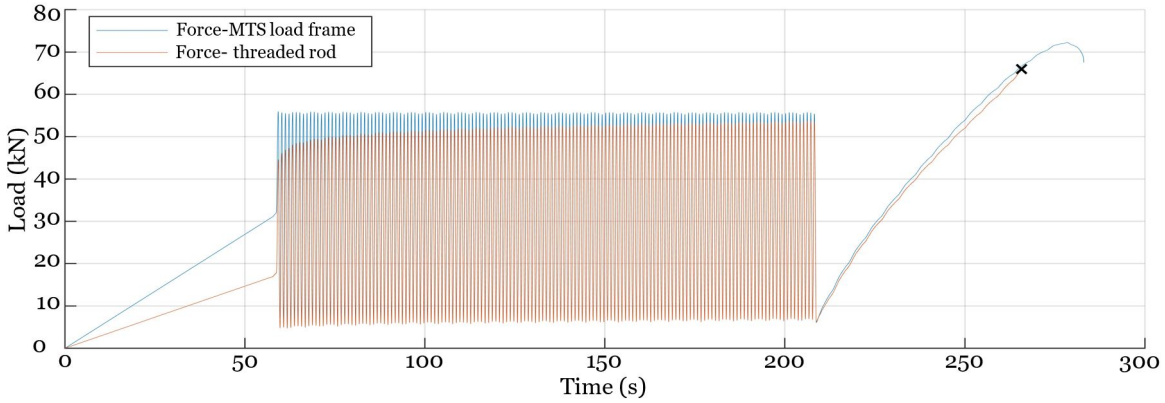

FIGURE 15
Load vs. time curves of anchorages without postinstalled reinforcing bars CL-S-03
Source: Own elaboration.

Figure 16 shows the load versus time curve for alternative CL-V-#3-C2-01, which illustrates the overall behavior of the system. In the first part of the test, where the anchorage is subjected to loading and unloading cycles, the threaded bar absorbs between 75 % and 85 % of the applied force, whereas the reinforcing bars absorb between 8.5 % and 12 %. In the second part of the test, where a monotonic test is performed, the postinstalled rebars gain strength as the force increases until they reach a maximum of 14.38 kN, which is 18 % of the applied force.

The postinstalled reinforcing bars reached a total force of 27 kN, which is 30 % of the total applied force. It is also observed that the force of the threaded bar reaches a maximum of 73.6 kN. A comparison of the results of the cyclic tests with those of the monotonic tests (Table 11) reveals that the maximum load of the cyclic tests increased by an average of 7.73 kN (9.8 %). This load increase is also evident in the tests performed by Hoehler and Eligehausen [22] for expansion anchors, where the load increase in cyclic tests with respect to monotonic tests was 2.35 kN (7.9 %). Similarly, Mahrenholtz et al. [10] reported a load increase of 4.8 kN (4.3 %) in cyclic tests compared with monotonic tests.

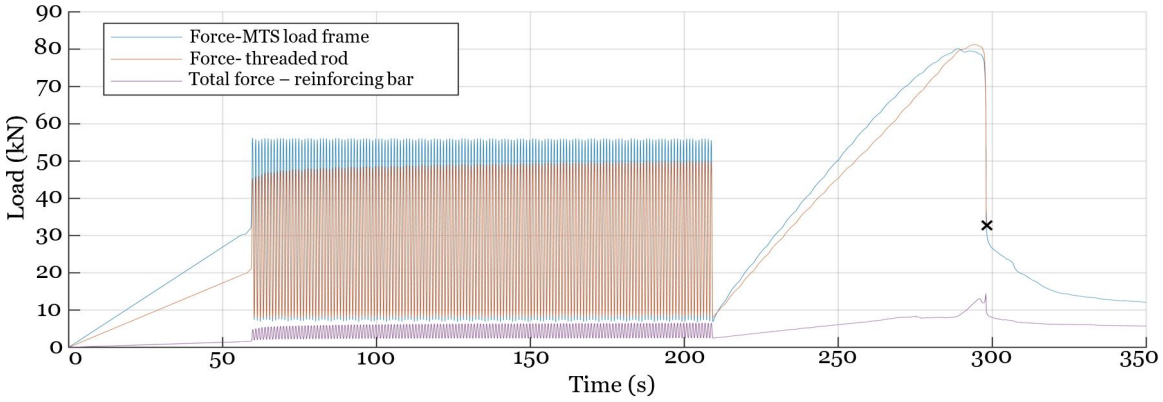

FIGURE 16
Load-time curves of the reinforced anchor with two #3 (3/8 in) reinforcing postinstalled bars vertically (CL-V-#3-C2-01
Source: Own elaboration.

Figure 17 shows the load versus time curve for alternative CL-A-#3-C4-03. In the first part of the test, the threaded bar absorbs between 80 % and 90 % of the applied force. In the second part of the test, as the test progressed, the postinstalled bars began to exert force when the applied load exceeded 60 kN.

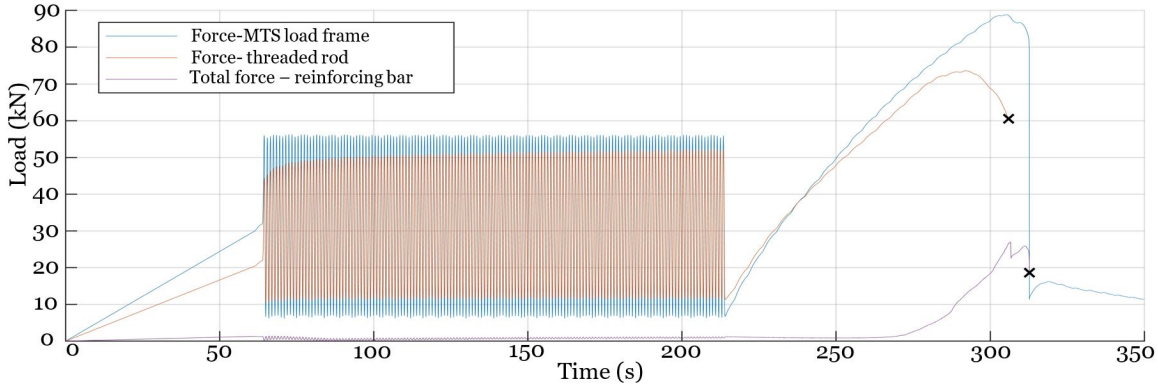

FIGURE 17
Load-time curves of anchorages reinforced with four #3 (3/8 in) reinforcing bars postinstalling at a 55° angle (CL-A-#3-C4-03)
Source: Own elaboration.

TABLE 11
Comparison of monotonic and cyclic test results

Code	Monotonic test		Cyclic test	
	Maximum load $N_{u\text{-}mo}$	Percentage change in load capacity $N_{c\ \%\text{-}mo}$	Maximum load $N_{u\text{-}cl}$	Percentage change in load capacity $N_{c\ \%\text{-}cl}$
CL-S	63.14	-	71.55	-
CL-V-#3-C2	73.86	17	80.75	12.9
CL-A-#3-C4	78.69	24.6	86.58	21

Source: Own elaboration.

Future Work

Our research will be expanded to include a larger number of samples and additional anchor configurations and installation conditions. Furthermore, the effects of aging, thermal cycling, and exposure to aggressive agents are incorporated. Additionally, with the results of the current and future research, analytical expressions and numerical models calibrated with the experimental results can be developed to predict the expected load increases for each configuration. Finally, the comprehensive analysis will result in the formulation of guidelines that will assist designers in the selection of epoxy-reinforced anchorage strategies that align with the specific loading and installation conditions.

Conclusions

1. The reinforcement of anchors with postinstalled reinforcing bars with the same embedment depth as the main anchor increases the anchor's bearing capacity by 9.4 % to 25 %.
2. The reinforcement alternative with four number 3 rebars installed at a drilling angle of 55° with respect to the surface (A-#3-C4) increases the load capacity by 25 % based on monotonic tensile tests and increases the load capacity by 21 % based on cyclic tensile tests. This reinforcement alternative exhibited the most favorable results.
3. The results of the monotonic tensile tests show that increasing the diameter or number of reinforcing bars installed increases the load capacity of the anchorage for the following reinforcement alternatives: four number three reinforcing bars installed vertically (M-V-#3-C4), two number four reinforcing bars installed vertically (M-V-#4-C2), two number three reinforcing bars installed at a drilling angle of 55° to the surface (M-A-#3-C2), two number four reinforcing bars installed at a drilling angle of 55° to the surface (M-A-#4-C3), two number three reinforcing bars installed at a drilling angle of 55° to the surface (M-A-#3-C2), two number four reinforcing bars installed at a drilling angle of 55° to the surface (M-A-#4-C2), and four number three reinforcing bars installed at a drilling angle of 55° to the surface (M-A-#3-C4). Similarly, the installation of reinforcing bars at a 55° angle provides greater load capacity to the anchorage than installing reinforcing bars vertically for the alternatives of four number three reinforcing bars installed at a 55° drilling angle to the surface (M-A-#3-C4) and four number four reinforcing bars installed at a 55° drilling angle to the surface (M-A-#4-C4).
4. The calculated efficiency (additional capacity/cost) enabled the identification of the optimal alternatives with the best use of resources in terms of additional capacity. The highest efficiency was achieved by the alternative of reinforcement with two number three reinforcing bars installed vertically (V-#3-C2), with an efficiency of 7,147 kN/USD.

5. Strain gages were used to determine the force absorbed by the threaded bar and the reinforcing bars, which helped to understand the anchorage behavior and the interaction of the reinforcement with the concrete.
6. A comparison of the results of the cyclic tests with those of the monotonic tests revealed that the maximum load of the cyclic tests exhibited an average increase of 7.73 kN (9.8 %). It was also shown that the loading and unloading cycles affected the distribution of internal forces in the steel bars of the reinforcement system.

Acknowledgments

The authors thank the School of Engineering Laboratories of the Pontificia Universidad Javeriana (Civil Engineering Laboratories, Materials and Civil Works) and all the technical staff where all the experimental tests were carried out, as well as the Vice President of Research of the Pontificia Universidad Javeriana for financing the project with ID 00007525. The research was also supported by HEIGHT ACCESS S.A.S., DIAMANTBEC/SIMPSON-Strong-Tie, CONCRETOS INDUSTRIALES S.A.S. and Red Expertos S.A.S. Finally, the authors thank Professor Daniela Carrasco Beltrán for the final proofreading.

References

[1] Mehmet Gesoglu, Turan Özturan, Melda Özel, y Erhan Güneyisi (2005). Tensile Behavior of Post-Installed Anchors in Plain and Steel Fiber Reinforced Normal- and High Strength Concretes. *ACI Struct J, vol. 102, pp. 224–231*. https://doi.org/10.14359/14273

[2] M. Philipp. (2012). Experimental Performance and Recommendations for Qualification of Post-installed Anchors for Seismic Applications. *Institut für Werkstoffe im Bauwesen der Universität Stuttgart*.

[3] N. Vita, A. Sharma, y J. Hofmann. (2019). *Local strengthening of anchorages with post-installed (supplementary) reinforcement*. En IOP Conference Series: Materials Science and Engineering. https://doi.org/10.1088/1757-899X/615/1/012093

[4] N. Vita, A. Sharma, y J. Hofmann. (2019). Strengthening of anchorages with post-installed supplementary reinforcement under shear loading. *Otto-Graf-Journal, vol. 18, 357–368*. https://www.mpa.uni-stuttgart.de/institut/publikationen/otto-graf-journal/new_downloadgallery/30_Vita.pdf

[5] American Concrete Institute. (2019). Building Code Requirements for Structural Concrete (ACI 318-19) and Commentary on Building Code Requirements for Structural Concrete (ACI 318R-19).

[6] N. Vita, A. Sharma, y J. Hofmann (2022). Bonded anchors with post-installed supplementary reinforcement under tension loading – Experimental investigations. *Eng Struct, vol. 252 https://doi.org/*10.1016/j.engstruct.2021.113754

[7] S. Mousavi, P. Jiradilok, K. Nagai, y R. Sahamitmongkol, (2020). Discrete mesoscale analysis of adhesive anchors under tensile load taking into account post-installed reinforcement. *Constr Build Mater, vol. 262*. https://doi.org/10.1016/j.conbuildmat.2020.120778

[8] S. Mousavi, Y. Seyed, y R. Sahamitmongkol. (2021). Post-installed anchors in concrete strengthened by post-installed reinforcement under tensile load. *European Journal of Environmental and Civil Engineering, Vol. 26, No. 13, 6563–6582*. https://doi.org/10.1080/19648189.2021.1948450

[9] S. Y. M. Siamakani, K. Nagai, P. Jiradilok, y R. Sahamitmongkol. (2022). Prevention of concrete breakout failure of expansion anchor in tension by post-installed reinforcement: Discrete analysis and experiment. *Case Studies in Construction Materials, vol. 17, p. e01233.* https://doi.org/10.1016/j.cscm.2022.e01233

[10] P. Mahrenholtz, R. Eligehausen, T. C. Hutchinson, y M. S. Hoehler. (2016). Behavior of postinstalled anchors tested by stepwise increasing cyclic load protocols. *ACI Struct J, vol. 113, No. 5, 997–1008.* https://doi.org/10.14359/51689023

[11] American Concrete Institute, ACI CODE-355.4-19 (Reapproved 2021). (2021). Qualification of Post-Installed Adhesive Anchors in Concrete and Commentary.

[12] ASTM International. (2022). ASTM E488/E488M-22 Standard Test Methods for Strength of Anchors in Concrete Elements.

[13] ASTM International. (2023). A193/A193M – 23 Standard Specification for Alloy-Steel and Stainless Steel Bolting for High-Temperature or High-Pressure Service and Other Special Purpose Applications.

[14] ASTM International. (2022). ASTM A706/A706M-22a Standard Specification for Deformed and Plain Low-Alloy Steel Bars for Concrete Reinforcement.

[15] ASTM International. (2022). ASTM E8/E8M-22 Standard Test Methods for Tension Testing of Metallic Materials.

[16] ASTM International. (2021). ASTM C39/C39M-21 Standard Test Method for Compressive Strength of Cylindrical Concrete Specimens.

[17] ICC-ES Evaluation Report ESR-4057. (2023). A Subsidiary of the International Code Council. https://icc-es.org/report-listing/esr-4057/

[18] Simpson Strong-Tie. (2023). Adhesive Anchoring Installation Instructions. Simpson Strong-Tie. Accessed: Oct. 02, 2023. https://www.strongtie.com/products/anchoring-systems/technical-notes/anchoring-adhesives/installation-instructions

[19] R. Eligehausen, R. Mallée, y J. F. S. Silva. (2006). Anchorage in Concrete Construction, vol. Primera Edición.

[20] Simpson Strong-Tie. (2023). Adhesive Cartridge Estimator. *Simpson Strong-Tie*. Accessed: Oct. 02, 2023. https://app.strongtie.com/ace?_ga=2.41083810.1889694015.1691092353-1986209455.1691092353

[21] Ministerio del Trabajo. República de Colombia. Mi Calculadora, *Ministerio del Trabajo*. Oct. 02, 2023. https://www.mintrabajo.gov.co/atencion-al-ciudadano/tramites-y-servicios/mi-calculadora

[22] Matthew S. Hoehler y Rolf Eligehausen. (2008). Behavior of Anchors in Cracked Concrete under Tension Cycling at Near-Ultimate Loads. *ACI Struct J*, pp. 601–608.

Notes

* Research article

How to cite this article: D. A. Espitia Rojas, Y. A. Alvarado Vargas, D. M. Ruiz Valencia, "Behavior of Adhesive Anchors Reinforced with Postinstalled Steel Bars under Monotonic and Cyclic Loading" Ing. Univ. vol. 28, 2024. https://doi.org/10.11144/Javeriana.iued28.baar